

# Wideband Nine-Port Reflectometer

Szczepan Odrobina, Kamil Staszek, Krzysztof Wincza, and Sławomir Gruszczynski

**Abstract**—The paper presents a wideband nine-port reflectometer realized as a cascade connection of six- and five-port reflectometers. It is shown that such a solution allows for a convenient adjustment of circuits' parameters in order to provide significantly reduced measurement uncertainty with respect to other reported reflectometers. Simultaneously, the proposed network features a simple and flexible design. For the experimental verification, the proposed nine-port reflectometer has been manufactured and incorporated into the system intended for reflection coefficient measurements within the frequency range 2.5 – 3.5 GHz. The obtained results are in an excellent agreement with the values measured using a commercial VNA.

**Keywords**—multiport measurement technique, reflectometer, reflection coefficient, measurement uncertainty, directional coupler, power divider, phase shifter

## I. INTRODUCTION

MULTI-PORT measurement technique is one of well-recognized areas in microwave engineering. Although invented as an alternative for large and complex vector network analyzers [1], today this technique finds a wide variety of applications, which make use of its simplicity, robustness, and low overall costs. In principle a multiport measurement system is composed of a signal source, a multiport power distribution network and power meters [2]. Such a structure makes multiport systems easily scalable to higher frequencies [3] and allows their miniaturization [4]. Due to an appropriate power distribution scheme, the measured power can be translated into complex reflection coefficient [5], target distance [6], or complex permittivity [7].

Among all multiport systems reported in literature, six-port ones are the most common, however, a higher number of ports can be utilized for measurement uncertainty decrease [8]. In [9] a ten-port reflectometer composed of appropriately connected three  $4 \times 4$  Butler matrices has been shown. The circuit is capable of a broadband operation, however, it suffers from a significant network complexity, since it is composed of twelve directional couplers and six phase shifters. Another interesting example of a ten-port reflectometer has been reported in [10]. It has been assembled using two classic six-port reflectometers proposed by G. F. Engen [1]. Their connection, however, is not planar and requires additional attenuators. Moreover, the

reflectometer contains two ports for reference power measurement, but only one is needed in measurement application. Due to the above facts this ten-port reflectometer is not efficient in terms of power consumption and occupied area.

In this paper, a wideband nine-port reflectometer overcoming the limitations of the aforementioned ten-port reflectometers is proposed. It is constituted by a cascade connection of a six-port reflectometer and a five-port reflectometer. Simultaneously, it features a lower number of required components such as directional couplers, power dividers, and phase shifters comparing to the other reported designs. An analysis of the measurement uncertainty is presented, on the basis of which, the reflectometer's parameters ensuring the minimum obtainable measurement uncertainty have been derived. The proposed nine-port reflectometer has been designed and optimized to operate within a broad frequency range from 2.5 to 3.5 GHz. The manufactured circuit has been incorporated into a measurement system and its performance has been validated in measurements of reflection coefficients of a series of reflective elements. It is shown that the obtained values are very close to the ones measured with the usage of a commercial vector network analyzer.

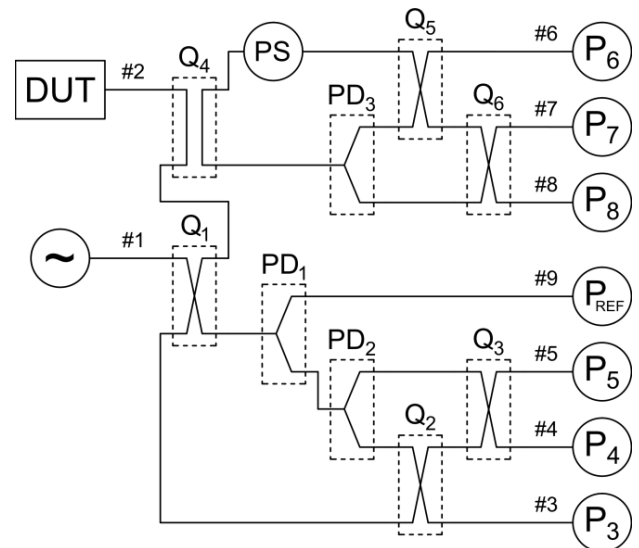


Fig. 1. A schematic diagram of the proposed nine-port reflectometer.

## II. THEORETICAL ANALYSIS

A schematic diagram of the proposed nine-port reflectometer is illustrated in Fig. 1. It is composed of coupled-line directional couplers  $Q_1 - Q_6$ , power dividers  $PD_1 - PD_3$ , and the phase shifter PS. The network is excited at port #1, Device Under Test

This work was supported by Dean's Grant no. 15.11.230.332.

The authors are with the AGH University of Science and Technology, Department of Electronics, Cracow, Poland (e-mails: szczepan.odrobina@agh.edu.pl, kamil.staszek@agh.edu.pl, krzysztof.wincza@agh.edu.pl, slawomir.gruszczynski@agh.edu.pl).

(the reflection coefficient of which is to be measured) is connected to port #2, and to the remaining ports #3 – #9 power meters are connected. Analyzing the network it can be observed that a signal incident at any of power meters  $P_3 – P_8$  is a sum of signal depending on the reflection coefficient  $\Gamma$  measured at port #2 and a reference signal. On the other hand, the power measured at port #9 does not depend on the measured reflection coefficient  $\Gamma$ , thus it can be utilized for normalization purpose. In the light of the above one can formulate a well-known relation between the measured reflection coefficient  $\Gamma$  and the measured power  $P_3 – P_8$  and  $P_{REF}$  [1]:

$$p_i = \frac{P_i}{P_{REF}} = q_i \left| \frac{1+A_i\Gamma}{1+A_0\Gamma} \right|^2 \quad (1)$$

where  $p_i$  ( $i = 3 – 8$ ) are the normalized power values, whereas  $q_i$ ,  $A_i$  and  $A_0$  are constants resulting from the measurement system topology and have to be determined utilizing an appropriate calibration procedure prior to reflection coefficient measurements.

It is worth mentioning that, although all multiport reflectometers can be described by (1), they differ in the number power ports with power meters connected and the values of system constants  $q_i$ ,  $A_i$  and  $A_0$ , which defines the uncertainty of reflection coefficient measurement [8]. In order to analyze performance of a given multiport reflectometer, one can use a geometrical interpretation of (1), according to which the complex reflection coefficient  $\Gamma$  is represented as a point of intersection of circles having centers  $c_i$  defined as [11]:

$$c_i = -\frac{1}{A_i} \quad (2)$$

whereas their radii  $R_i$  are equal to:

$$R_i = \sqrt{\frac{p_i}{q_i|A_i|^2}} \quad (3)$$

It can be concluded that the circle centers distribution, i.e. arrangement of points  $c_i$  is an inherent feature of a reflectometer, and the radii  $R_i$  depend on the measured power. As it has been shown in [8], the mutual location of circle centers significantly affects the measurement conditions and allows for the measurement uncertainty estimation. It is crucial, therefore, to design a reflectometer featuring circle centers' distribution ensuring minimized reflection coefficient measurement uncertainty. To derive circle centers' distribution for the proposed nine-port, the following analysis can be conducted.

As it can be observed in Fig. 1, the proposed nine-port reflectometer is composed of a six-port reflectometer connected in cascade with a five-port reflectometer. The mentioned six-port is realized by the directional couplers  $Q_1 – Q_3$  and power dividers  $PD_1 – PD_2$ . As it can be seen, the components  $PD_2$ ,  $Q_2$  and  $Q_3$  form a signal correlator applied in recently reported six-port reflectometer providing an enhanced measurement uncertainty [12]. Assuming an equal power split of  $PD_2$  and the coupling coefficients of  $Q_2$  and  $Q_3$  being equal to 4.77 dB and 3 dB respectively, the correlator ensures a uniform distribution of three circle centers  $c_3 – c_5$  (corresponding to ports #3 – #5) having equal magnitude with angular separation of  $120^\circ$ . Moreover, the magnitude  $|c_A| = |c_3| = |c_4| = |c_5|$  can be adjusted by a choice of the coupling coefficient of  $Q_1$  and power split

ratio of  $PD_1$ . Furthermore, the port of  $Q_1$  being coupled with respect to the excitation port #1 is connected to another reflectometer composed of directional couplers  $Q_4 – Q_6$ , power divider  $PD_3$  and phase shifter PS. It must be underlined that the components  $PD_3$ ,  $Q_5$  and  $Q_6$  form exactly the same correlator as the one mentioned above, however, the magnitude  $|c_B| = |c_6| = |c_7| = |c_8|$  is not equal to  $|c_A|$  and depends on the coupling coefficients of the couplers  $Q_1$  and  $Q_4$ . It is worth noting that the coupler  $Q_4$  realized without crossing ensures a planar structure of the entire nine-port reflectometer with no internal ports. Additionally, the phase shifter PS allows for rotating the circle centers distribution  $\{c_6, c_7, c_8\}$  with respect to circle centers distribution  $\{c_3, c_4, c_5\}$ .

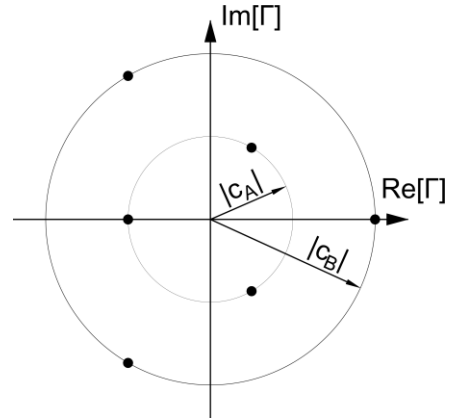


Fig. 2. An ideal circle centers distribution of the proposed broadband nine-port reflectometer.

As a result one can obtain the overall circle centers distribution composed of six points with the angle between two adjacent points of  $60^\circ$  and interchanging magnitudes  $|c_A|$  and  $|c_B|$ , as shown in Fig. 2.

### III. SYNTHESIS OF THE NINE-PORT FEATURING AN OPTIMAL CIRCLE CENTERS DISTRIBUTION

As it has been shown in the previous section, the proposed nine-port reflectometer features circle centers distribution composed of two triples of points on a complex plane  $\{c_3, c_4, c_5\}$  and  $\{c_6, c_7, c_8\}$  having magnitudes  $|c_A|$  and  $|c_B|$ , respectively. These magnitudes can be adjusted by choosing coupling coefficients of the couplers  $Q_1$  and  $Q_4$  and power split of power divider  $PD_1$ . Since the measurement uncertainty of multiport reflectometers in general strongly depends on circle centers distribution, it is crucial to determine the magnitudes  $|c_A|$  and  $|c_B|$  ensuring the minimum measurement uncertainty for the measured reflection coefficient  $\Gamma$ . For this purpose the method reported in [8] and [13] has been applied, which allows for estimation of the maximum measurement error for all reflection coefficients fulfilling  $|\Gamma| \leq 1$ , basing on the power measurement uncertainty of the power meters and circle centers distribution of the proposed nine-port reflectometer.

In that method, the measurement error is defined as the distance on the complex plane between the genuine and measured values of  $\Gamma$ . The magnitudes  $|c_A|$  and  $|c_B|$  have been swept in the range from 0.4 to 1.4, and for each set of these two values, the maximum error distribution for all complex

reflection coefficients having the magnitudes not exceeding 1 has been calculated. Moreover, the power measurement uncertainty has been assumed to be  $\pm 0.1$  dB.

Further, from each maximum error distribution for a given set  $\{|c_A|, |c_B|\}$ , the maximum value has been taken to create a map relating these magnitudes and the maximum measurement error obtainable for all reflection coefficients satisfying condition  $|\Gamma| \leq 1$ .

The achieved results are illustrated in Fig. 3. It can be observed that the optimum performance of the proposed nine-port reflectometer can be obtained for the magnitudes equal to 0.65 and 1.0. It should be emphasized that these both possible scenarios, i.e.  $|c_A| = 0.65$  and  $|c_B| = 1.0$ , as well as  $|c_A| = 1.0$  and  $|c_B| = 0.65$  are equivalent, since the only difference is a rotation of the entire circle centers distribution by  $60^\circ$ , which has no impact on the maximum measurement error value. Hence, ensuring the above magnitudes, the maximum measurement error does not exceed the value of 0.0157. Moreover, it can be observed that if one magnitude is equal to 0.65, the second magnitude can take a value between 0.65 – 1.4 and the maximum measurement error will not exceed 0.0159. Therefore, requirements related to the higher magnitude are relaxed. The maximum measurement error distribution for  $|c_A| = 0.65$  and  $|c_B| = 1.0$  is shown in Fig. 4a.

Furthermore, to clearly show the advantageous performance of the proposed nine-port reflectometer featuring the investigated circle centers distribution, the above described procedure has been applied to estimate the maximum measurement error for two six-port reflectometers featuring circle centers distributions composed of only three uniformly distributed points with the magnitude of 0.65, and 1.0. The corresponding maximum measurement error distributions are presented in Fig. 4b and Fig. 4c, respectively. It can be observed that the proposed nine-port reflectometer provides the maximum measurement error being more than 2.5 times lower than the corresponding values for considered six-port reflectometers.

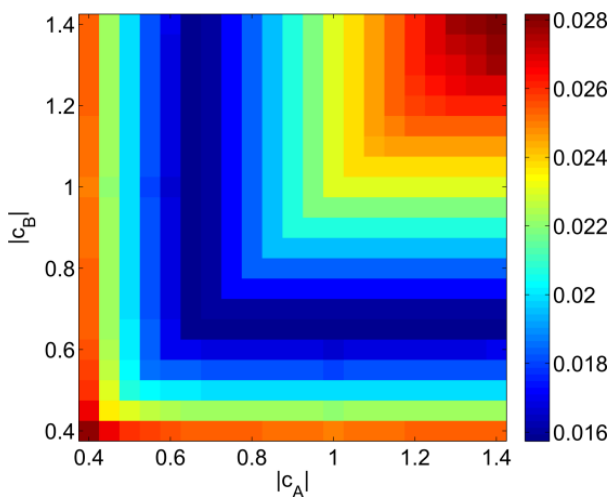


Fig. 3. The maximum measurement error for all reflection coefficients  $\Gamma$  having the magnitudes not exceeding 1 vs. the magnitudes  $|c_A|$  and  $|c_B|$ . The assumed power measurement uncertainty is equal to  $\pm 0.1$  dB.

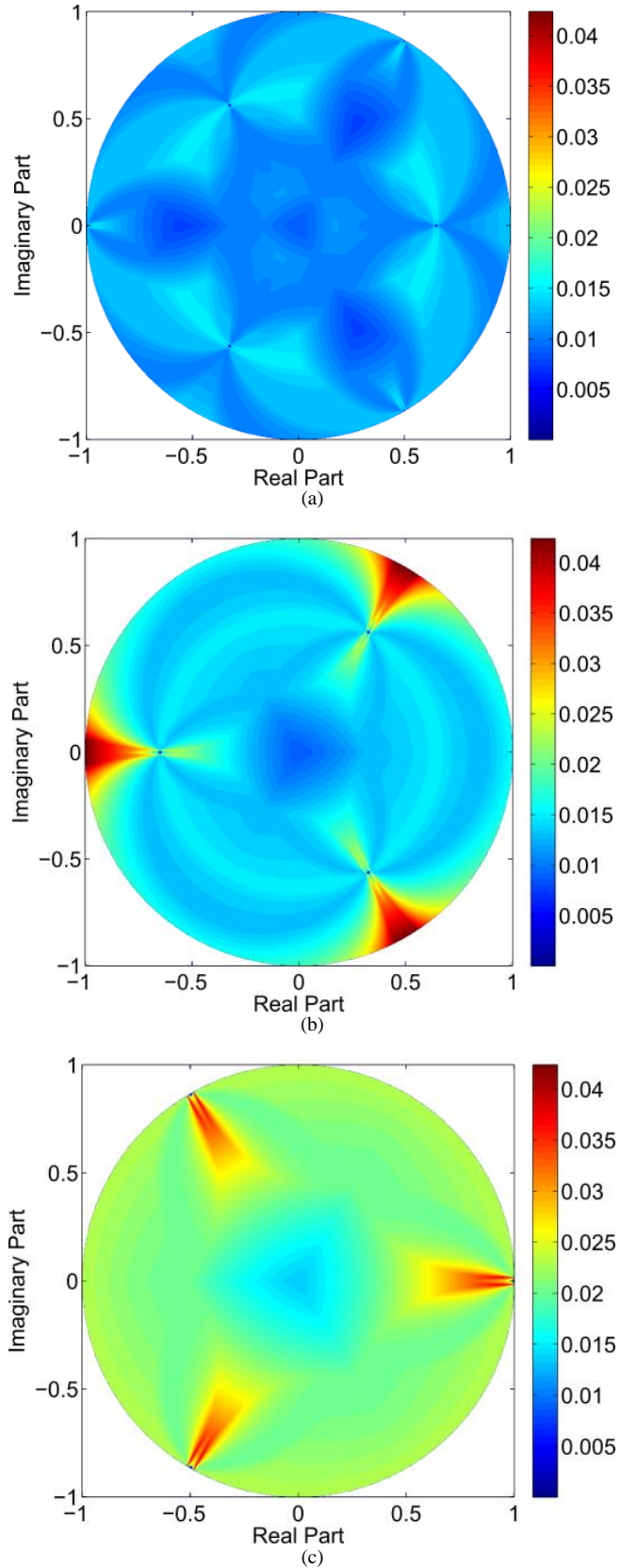


Fig. 4. The maximum measurement error distribution of the proposed nine-port reflectometer for  $|c_A| = 0.65$  and  $|c_B| = 1.0$  (a), the maximum measurement error for a six-port reflectometer featuring circle centers distributions composed of only three uniformly distributed points with the magnitude of 0.65 (b), and 1.0 (c).

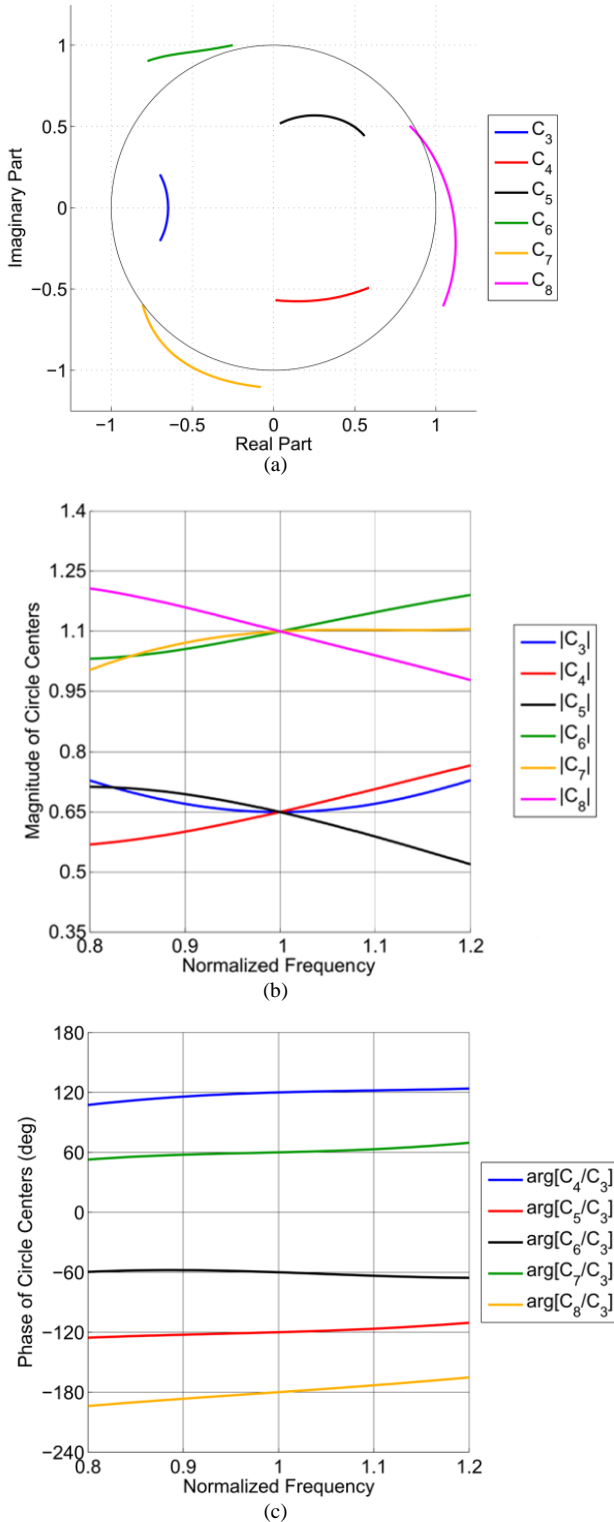


Fig. 5. An ideal circle centers distribution of the proposed reflectometer vs. frequency, in which  $Q_1 - Q_6$  are single-section coupled-line directional couplers,  $PD_1 - PD_3$  are Wilkinson power dividers, and PS is an ideal  $60^\circ$  phase shifter. General view on the complex plane (a), magnitude of circle centers (b), and differential phases of circle centers (c).

The above analysis has revealed the optimum circle centers distribution of the proposed nine-port reflectometer. In order to ensure the derived magnitudes  $|c_A|$  and  $|c_B|$ , the coupling coefficients of the couplers  $Q_1$  and  $Q_4$ , as well as power split of the power divider  $PD_1$  must be appropriately chosen. As seen,

one degree of freedom exists, hence, the coupling coefficient of coupler  $Q_1$  has been chosen to be the same as in case of the couplers  $Q_3$ , and  $Q_6$  featuring coupling coefficient of 3 dB. Therefore, to provide  $|c_A| = |c_3| = |c_4| = |c_5| = 0.65$ , the transmission coefficient of  $PD_1$  between its ports connected to  $Q_1$  and  $PD_2$  must be equal to  $-8.4$  dB. Since  $PD_1$  is assumed to be a lossless power divider, the remaining power is transmitted to port #9 of the nine-port reflectometer as the reference power  $P_{REF}$ .

Analyzing the schematic diagram presented in Fig. 1, it can be shown that to obtain  $|c_B| = |c_6| = |c_7| = |c_8| = 1.0$ , the coupling coefficient of  $Q_4$  should be 0 ( $-\infty$  dB), which would not lead to a feasible reflectometer design. However, as seen in Fig. 3, the magnitude  $|c_B|$  can be changed within a certain range with a negligible impact on the overall measurement uncertainty. Therefore,  $|c_B|$  has been assumed to be 1.1, which is obtained if the coupling coefficient of  $Q_4$  is equal to 7.6 dB. Fig. 5 presents an ideal circle centers distribution of the proposed reflectometer vs. frequency, in which  $Q_1 - Q_6$  are single-section coupled-line directional couplers,  $PD_1 - PD_3$  are Wilkinson power dividers, and PS is an ideal  $60^\circ$  phase shifter. A uniform mutual arrangement of circle centers  $c_i$  in terms on magnitude and differential phase over a wide frequency range is seen.

#### IV. DESIGN OF THE WIDEBAND NINE-PORT REFLECTOMETER

The proposed nine-port reflectometer has been designed in a symmetrical stripline structure composed of three layers of ARLON 25N laminate, as shown in Fig. 6, for the center frequency equal to 3 GHz. For a realization of 3-dB couplers ( $Q_1$ ,  $Q_3$ , and  $Q_6$ ) and 4.77-dB couplers ( $Q_2$  and  $Q_5$ ), the single-section coupled-line directional couplers reported in [12] have been utilized. The equal power split power dividers  $PD_2$  and  $PD_3$  have been designed as Wilkinson power dividers. Due to the excitation of these dividers only at port from which the power is equally split, the isolating resistors have been omitted, what has not influenced the impedance matching at ports #1 and #2. Further, the directional coupler  $Q_4$  has also been designed as a single-section coupled-line directional coupler with the coupling coefficient of 7.6 dB. As described in Section II, this coupler has been designed without crossing in order to provide port #2 at the outside of the circuitry for a convenient DUT connection. The power divider  $PD_1$ , due to its unequal power split, has been designed as a single-section coupled-line directional coupler featuring the coupling coefficient of 8.4 dB with the port being isolated with respect to the excitation port left open. Finally, the phase shifter PS has been designed as a single-section Schiffman phase shifter.

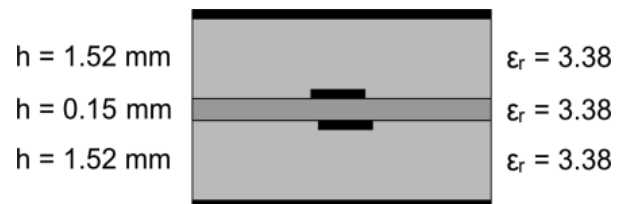


Fig. 6. Cross-sectional view of the stripline structure, in which the proposed wideband nine-port reflectometer has been designed.

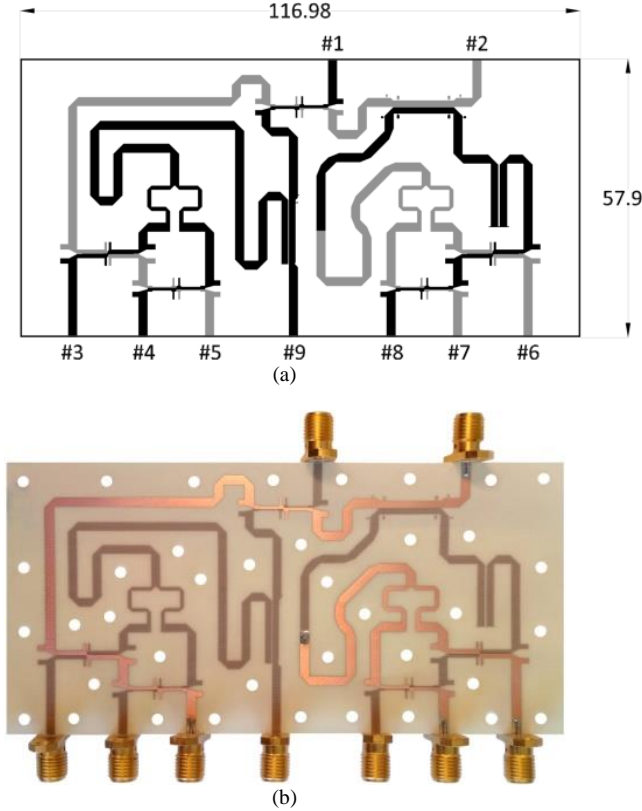


Fig. 7. Layout of the nine-port reflectometer (a) and a photograph of the inner laminate on which the metallization layers have been etched (b).

All the components have been connected with transmission lines, the lengths of which additionally compensate differences in the physical dimensions of particular components. The layout of the entire nine-port reflectometer and a photograph of the inner laminate, on which the metallization layers have been etched, are shown in Fig. 7.

The electromagnetic simulation of the designed broadband nine-port reflectometer has been done with the aid of *NI AWR Design Environment* software. Further, the reflectometer has been manufactured and its  $S$ -parameters have been measured using N5224A Vector Network Analyzer by Keysight. The EM calculated and measured scattering parameters being the most crucial from the point of view of reflection coefficient measurements are plotted in Fig. 8. As seen, the manufactured nine-port reflectometer features a good impedance match and flat frequency responses over the bandwidth 2.5 – 3.5 GHz, therefore, this interval has been assumed to be the operational bandwidth of the developed reflectometer.

## V. CALIBRATION & MEASUREMENTS

The manufactured nine-port reflectometer has been incorporated into a measurement system excited with the use of Rohde & Schwarz SMB 100A swept oscillator providing a 10-dBm signal. For power measurements, seven power meters PWR-8FS by Mini-Circuits have been used. They feature the measurement uncertainty  $\pm 0.1$  dB within the power range from -30 dBm to +20 dBm. A photograph of the entire measurement system is shown in Fig. 9. Further, the system has been calibrated following the procedure described in [14] with the use of several known reflection coefficients. As a result, the system

constants  $q_i$ ,  $A_i$  and  $A_0$  occurring in (1) have been defined. Using (2), the circle centers  $c_i$  have been derived and plotted in Fig. 10.

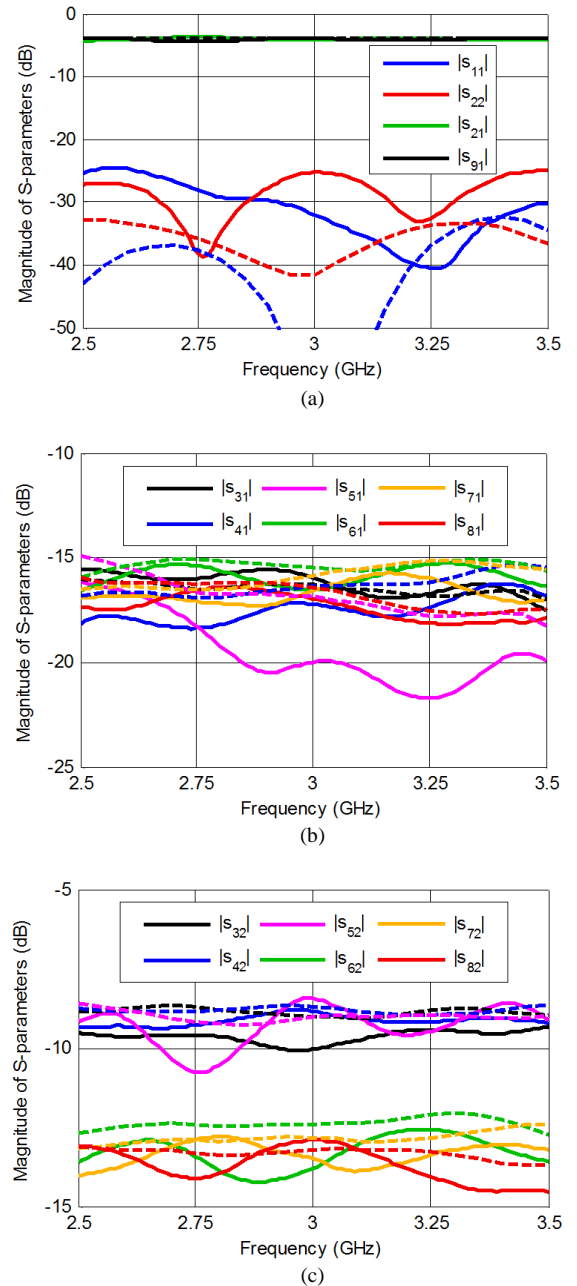


Fig. 8. The  $S$ -parameters of the manufactured nine-port reflectometer (solid lines: measurement results, dashed lines: electromagnetic simulation results). Magnitudes of reflection coefficients and transmission coefficients from port #1 to port #2 and port #9 (a). Magnitudes of transmission coefficients to ports with power detectors connected: from port #1 (b), from port #2 (c).

As it can be observed, the developed system features the mutual arrangement clearly corresponding to the theoretical one, ensuring advantageous measurement conditions. To examine performance of the proposed nine-port reflectometer, a set of reflective elements has been chosen to be measured with the use of the developed system and using a commercial VNA N5224A by Keysight for a comparison. These elements have been realized as broadband SMA attenuators, terminated with open-circuit, with insertion loss taking values equal to -1 dB, -2 dB, -3 dB, -6 dB, -10 dB, -13 dB, -16 dB, and -20 dB, providing the

reflection coefficients' magnitudes -2 dB, -4 dB, -6 dB, -12 dB, -20 dB, -26 dB, -32 dB, and -40 dB, respectively. The reflection coefficients measured utilizing the developed system are illustrated in Fig. 11. Due to very similar phase responses, the phase characteristics have been shown for the highest and the lowest magnitude of the reflection coefficient. Further, the same elements have been measured with the aid of VNA. The measurement error, defined as a difference between the values measured using the proposed nine-port reflectometer and those measured with the aid of VNA are shown in Fig. 12.

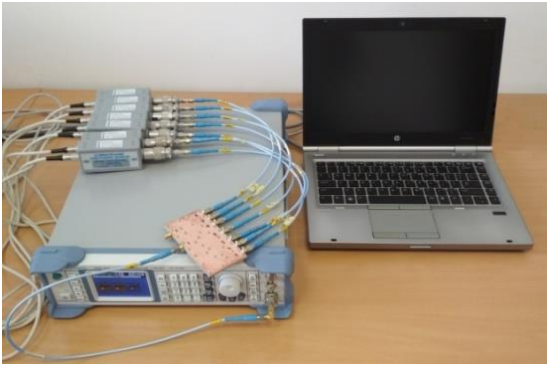


Fig. 9. A photograph of the developed measurement system incorporating the proposed nine-port reflectometer.

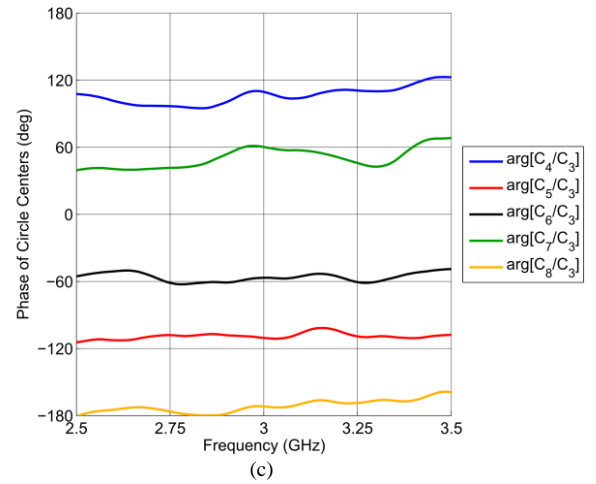
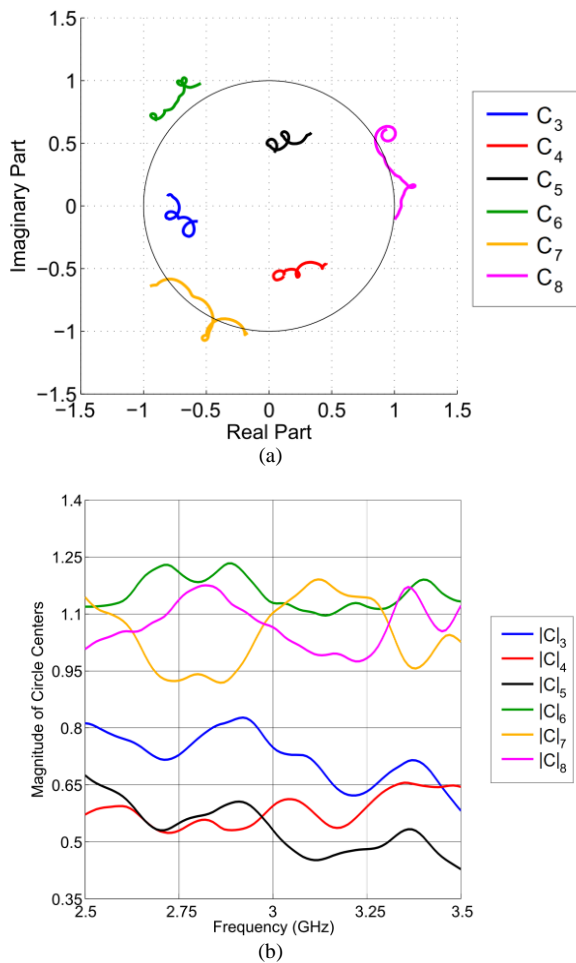


Fig. 10. Circle centers distribution of the developed measurement system as a result of the calibration procedure: general view on the complex plane (a), magnitude of circle centers (b), and differential phases of circle centers (c).

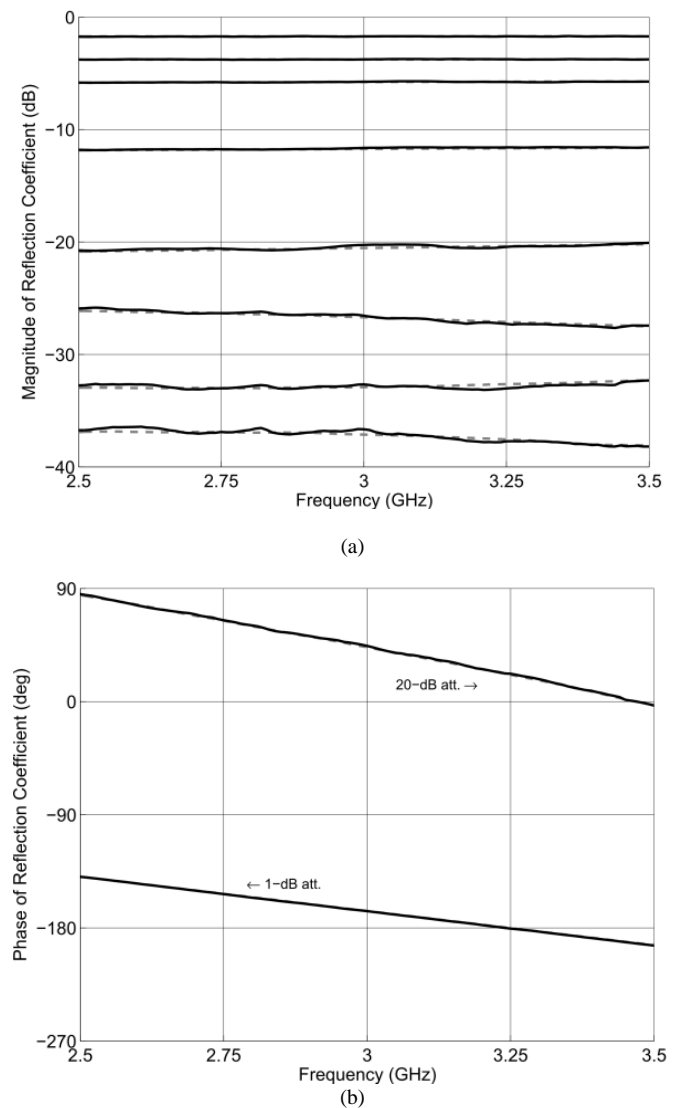


Fig. 11. Reflection coefficients of reflective elements realized as broadband SMA attenuators, terminated with open-circuit: magnitude (a) and phase (b).

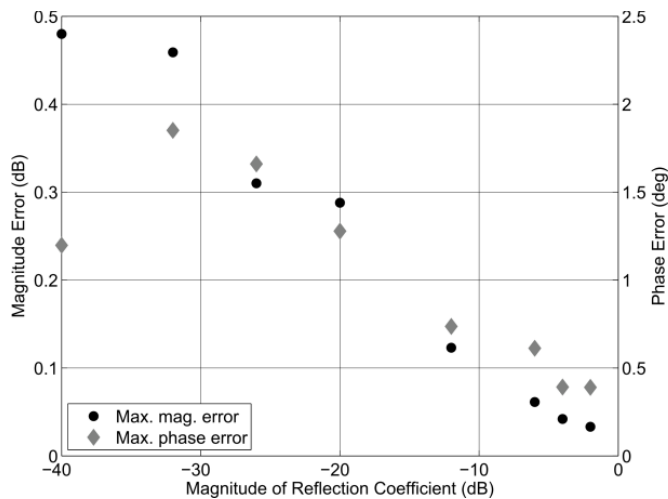


Fig. 12. Measurement error, defined as a difference between the values measured using the proposed nine-port reflectometer and those measured with the aid of VNA: magnitude error and phase error.

As it can be observed, the developed measurement system allows for precise reflection coefficient measurements within the entire operational frequency range.

## VI. CONCLUSIONS

In this paper, a nine-port reflectometer capable of wideband operation has been presented. It is composed of six-port reflectometer and five-port reflectometer connected in cascade, providing advantageous conditions for reflection coefficient measurements, and simultaneously featuring a simple topology. The presented analysis has allowed for derivation of optimal parameters ensuring the minimum measurement uncertainty, which is more than two times lower than the measurement uncertainty of six-port reflectometers. The proposed nine-port reflectometer has been designed, manufactured, and applied in the system intended for measurements of reflection coefficients within a wide frequency range 2.5 – 3.5 GHz. For an experimental verification, the developed nine-port reflectometer has been utilized to measure reflection coefficients of several reflective elements, the magnitudes of which cover the range from -40 dB to -2 dB. The obtained results have been compared to the values gained with the use of a commercial VNA, showing an excellent agreement in terms of magnitude and phase.

## REFERENCES

- [1] G. F. Engen, "The six-port reflectometer: An alternative network analyzer," *IEEE Trans. Microw. Theory Techn.*, vol. 25, no. 12, pp. 1075-1080, Dec. 1977.
- [2] G. F. Engen, "A (historical) review of the six-port measurement technique," *IEEE Trans. Microw. Theory Techn.*, vol. 45, no. 12, pp. 2414-2417, Dec. 1997.
- [3] B. Laemmle, K. Schmalz, C. Scheytt, D. Kissinger, and R. Weigel, "A 122 GHz multiprobe reflectometer for dielectric sensor readout in SiGe BiCMOS technology," in Proc. of *Compound Semiconductor Integrated Circuit Symposium (CSICS)*, Waikoloa, USA, Oct. 2011, pp. 1 - 4.
- [4] R. G. Venter, R. Hou, K. Buisman, M. Spirito, K. Werner and L. C. N. de Vreede, "A package-integratable six-port reflectometer for power devices," *Int. Microw. Symp. IMS 2014*, Tampa, USA, 2014, pp. 1-4.
- [5] K. Haddadi, T. Lasri, "Formulation for complete and accurate calibration of six-port reflectometers," *IEEE Trans. Microw. Theory Techn.*, vol. 60, no. 3, pp. 574-581, March. 2012.
- [6] F. Barbon, G. Vinci, S. Lindner, R. Weigel, and A. Koelpin, "A six-port interferometer based micrometer-accuracy displacement and vibration measurement radar," in Proc. of *Int. Microw. Symp. IMS 2012*, Montreal, Canada, June 2012, pp. 1-3.
- [7] K. Kim, N. Kim, S-H. Hwang, Y-K. Kim, and Y. Kwon, "A miniaturized broadband multi-state reflectometer integrated on a silicon MEMS probe for complex permittivity measurement of biological material," *IEEE Trans. Microw. Theory Techn.*, vol. 61, no. 5, pp. 2205-2214, May 2013.
- [8] K. Staszek, S. Gruszczynski, and K. Wincza, "Theoretical limits and accuracy improvement of reflection coefficient measurements in six-port reflectometers," *IEEE Trans. Microw. Theory Techn.*, vol. 61, no. 8, pp. 2966-2974, August 2013.
- [9] K. Staszek, S. Gruszczynski, and K. Wincza, "Broadband ten-port reflectometer with enhanced measurement accuracy," in Proc. of *16th IEEE Wireless and Microwave Technology Conference*, Cocoa Beach, United States 2015, pp. 1-4.
- [10] A. Askarian, G. Moradi, "Ultra wideband microwave ten-port reflectometer," *Appl. Comput. Electron.*, vol. 30, no. 1, pp. 61-67, January 2015.
- [11] K. Staszek, S. Gruszczynski, and K. Wincza, "Measurement accuracy enhancement in six-port reflectometers," *IEEE Microw. Wireless Compon. Lett.*, vol. 25, no. 8, pp. 553-555, August 2015.
- [12] K. Staszek, S. Gruszczynski, and K. Wincza, "Six-port reflectometer providing enhanced power distribution," *IEEE Trans. Microw. Theory Techn.*, vol. 64, no. 3, pp. 939-951, March 2016.
- [13] K. Staszek, S. Gruszczynski, and K. Wincza, "Design and accuracy analysis of a broadband six-port reflectometer utilizing coupled-line directional couplers," *Microw. Opt. Technol. Lett.*, vol. 55, no. 7, pp. 1485-1490, July 2013.
- [14] K. Staszek, P. Kaminski, A. Rydosz, S. Gruszczynski, and K. Wincza, "A least-squares approach to the calibration of multipoint reflectometers", in Proc. of *Int. Microw. & RF Conf.*, Delhi, India 2013, pp. 1-4.